SIN-CHN SCIENTIFIC PRESS PTE.LTD.

Molecular & Cellular Biomechanics 2025, 22(4), 1404.
https://doi.org/10.62617/mcb1404

Article

Optimization of working efficiency of rape crawler mower header in agricultural machinery cooperatives based on biomechanics

Xieraili Tuerjun[1], Junxian Guo[1,*], Jungui Ma[2]

[1] Xinjiang Agricultural University, Urumqi 830052, China
[2] Xinjiang Agricultural and Rural Mechanization Development Center, Urumqi 830054, China
*** Corresponding author:** Junxian Guo, alialijun9810@163.com

CITATION

Tuerjun X, Guo J, Ma J. Optimization of working efficiency of rape crawler mower header in agricultural machinery cooperatives based on biomechanics. Molecular & Cellular Biomechanics. 2025; 22(4): 1404. https://doi.org/10.62617/mcb1404

ARTICLE INFO

Received: 20 January 2025
Accepted: 20 February 2025
Available online: 4 March 2025

Abstract: This paper focuses on the optimization of operation efficiency of rape crawler mower header in Agricultural Machinery Cooperatives. In view of the important position of rape in agriculture and the problems existing in the cutting, conveying and laying of the existing windrower header, biomechanical methods were introduced. The working principle, structure and main parameters of the windrower are introduced in detail. The biomechanical analysis of the header operation process is carried out, and the key components such as reel, cutter and conveyor are designed and optimized. The header device frame topology is also optimized. The results showed that the first three natural frequencies of the header were increased after optimization, which effectively avoided the resonance risk, and the amplitudes of monitoring points in vibration test were significantly reduced, indicating that the optimization strategy was effective, which was of great significance to improve the efficiency and quality of rape harvest and promote the development of agricultural mechanization.

Keywords: rape; crawler windrower; biomechanics; header efficiency optimization; topological optimization

1. Introduction

As a vital oil crop in China, rapeseed occupies a pivotal position in the field of agricultural production. According to relevant data, China's rape planting area is extensive, and the annual yield is also considerable, which plays an irreplaceable role in ensuring the safety of national edible oil supply [1]. Rapeseed is not only the main source of edible oil, but also has important applications in industry, medicine and other fields. Its industrial chain covers planting, processing, sales and other links, which is of great significance to promote the development of rural economy and increase farmers' income. In the harvesting process of rape, mechanized operation has become a key means to improve efficiency and reduce costs [2]. With its good trafficability, stability and adaptability to complex terrain, crawler windrower has been widely used in rape harvesting [3]. However, at present, there are still many problems to be solved in the header operation efficiency of rape crawler mower. For example, during the cutting process, the cutting is often not smooth and the stem is seriously broken, which not only leads to the increase of rapeseed loss, affects the economic benefits of farmers, but also reduces the quality of rapeseed, which is not conducive to subsequent processing and sales.

As an interdisciplinary subject integrating biology and mechanics, biomechanics provides a new idea and method for solving the problem of cutting efficiency of rape crawler mower [4]. Through in-depth study of the biomechanical

properties of rape in the process of cutting, conveying and laying, we can accurately grasp the key information of rape, such as the stress situation, deformation law and motion trajectory [5]. Based on this information, we can optimize the structural parameters of the header, such as the shape, size and cutting angle of the cutter, and the speed, height and position of the reel, so as to make the structure of the header more in line with the biomechanical characteristics of rape, so as to improve the cutting efficiency and reduce the loss of rapeseed. This is of great significance to improve farmers' enthusiasm for planting rape and ensure the stable development of rape industry. In the field of rapeseed crawler mower header related research, many scholars have carried out exploration in the past. Early studies focused on the design and improvement of the basic structure of the header, such as improving the conveying smoothness of rape by adjusting the gear ratio of the header transmission system [6], but only from the perspective of mechanical transmission, did not fully consider the impact of rape's own biological characteristics on the operation. With the development of technology, some researches begin to pay attention to the influence of operation parameters on header efficiency. By exploring the relationship between reel speed, cutting speed and operation efficiency, it is found that reasonable matching parameters can improve efficiency [7], but the biomechanical response mechanism of rape behind parameter changes is not deeply analyzed, so it is difficult to achieve precise optimization.

Improving the operation efficiency of rape crawler windrower header is helpful to promote the development and progress of rape mechanized harvesting technology, improve the level of Agricultural Mechanization in China, and promote the construction of agricultural modernization.

2. Materials and methods

2.1. Working principle and structure of rape windrower

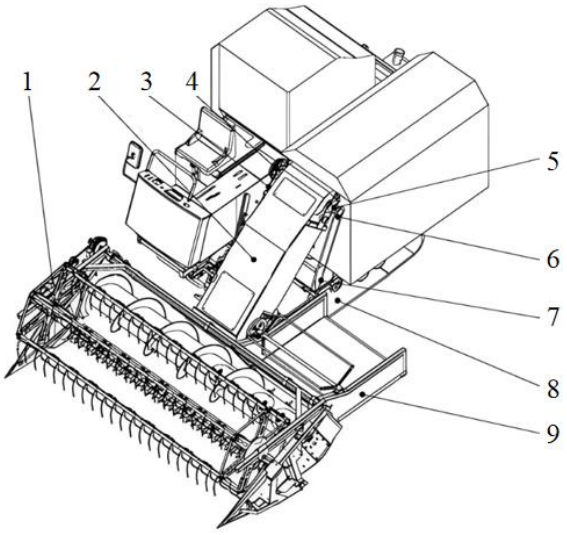

1. Pulling wheel 2. Rotating hydraulic cylinder 3. Contraction hydraulic cylinder 4. Hydraulic folding device 5. Conveyor bracket 6. Hydraulic ear shaft 7. Longmen frame 8. Track chassis 9. Cutting rack

Figure 1. Schematic diagram of the sun cutting machine.

The rape crawler windrower adopts the middle strip laying mode. The main structure of the whole machine is composed of hydraulic system, power chassis system and two rotatable folding header systems. The header system is composed of conveying device, cutting device, reel device and other transmission components. The specific structure model of the whole machine is shown in **Figure 1**.

The working principle of rape crawler windrower is to provide stable walking power through the crawler, so that the windrower can move flexibly in the field [8]. The cutting table, the core component of the windrower, is responsible for the cutting, conveying and laying of rape. In the process of operation, the windrower moves forward along the predetermined path, and the header will start to harvest the rape. According to the rape harvest requirements and the technical points of the windrower, the main technical parameters of the windrower are determined as shown in **Table 1**.

Table 1. Main parameters of tracked sun cutting machine.

Parameter	Value	Unit
Expand size (length × width × height)	5450 × 4300 × 2520	mm
Folding size (length × width × height)	5450 × 4300 × 2520	mm
Cutting width	4000	mm
Whole machine quality	4000	Kg
Auxiliary power	72	kW
Homework speed	0.8–1.1	$m.s^{-1}$
Homework efficiency	17.3–23.8	$mu.h^{-1}$
Cutting height	300–400	mm
Width of single-sided paving channel	700	mm
Laying channel height	650	mm

2.2. Biomechanical analysis of header operation process

In the harvesting link of the header, the mechanical interaction occurs between the reel and the rape plant [9]. When the reel rotates, the reel will exert a thrust on the rape plant, and the magnitude and direction of the thrust are crucial to the guiding effect of rape. If the reel speed is too fast and the thrust is too large, the rape plant may be pushed down or broken; If the rotation speed is too slow and the thrust is insufficient, the rape cannot be effectively guided to the cutter [10]. In the process of rotation, the reel will also be subject to the reaction force of rape plants. This reaction force will make the reel vibrate and wear, affecting the service life and working stability of the reel. By measuring the stress-strain curves of different parts of rape plants, we can accurately grasp its mechanical properties, so as to provide a scientific basis for determining the optimal speed, installation height and angle of reel.

The biomechanical analysis of cutting link is mainly based on the shear strength theory of materials. The cutting of Rape Stalk by the cutter is essentially a process in which the cutting force overcomes the shear strength of the stalk. According to the formula of material mechanics, the cutting force is closely related to the sharpness of the cutter blade, the cutting angle, and the diameter and material of the rape stem. The sharp blade can cut off the stem under a small cutting force, reducing energy consumption and stem breakage. The shear strength of different varieties of rape stems

was measured by experiment, and the stress distribution of stems under different cutting parameters was analyzed by finite element simulation, so as to optimize the design of the cutter.

In the conveying link, the motion and force of rape on the conveyor belt are analyzed by using the principles of motion mechanics and tribology. In order to ensure the smooth transportation of rape, the linear speed of the conveyor belt and the forward speed of the unit need to maintain an appropriate proportion, which is based on the consideration of the motion trajectory and inertia of rape. In addition, through tribological research, appropriate conveyor belt surface material and tine shape were selected to increase friction and prevent rape from slipping or accumulating during transportation.

2.3. Design and analysis of key components

2.3.1. Design of reel

The reel in the windrower is mainly responsible for the accurate guidance and support of the rape, so as to realize the effective push of the cut rape to the conveying system. In this design, an eccentric reel with a length of 2 m and a radius of 0.45 m, which is highly adaptable to crops, is selected. Referring to the agricultural machinery design guide, set the speed of the unit to keep at 1 m/s, and assume the λ value is 1.6. According to this, the motion trajectory equation of the reel is obtained as follows:

$$\lambda = \frac{v_b}{v_m} = \frac{\pi R_b n_b}{30 v_m},$$

where v_b is the circumferential speed of reel, m/s; v_m is the operating speed of the unit, 1m/s; R_b is the reel radius, 0.45 M; n_b is reel speed, r/min.

The calculated reel speed n_b = 42.5 r/min, reel circumferential speed v_b = 1.6 m/s. During the cutting and drying operation, in order to ensure that the reel should be vertically inserted into the plant when feeding, its installation height should meet the following requirements:

$$H_b = h_1 - h_0 + \frac{R_b}{\lambda},$$

where H_b is the installation height of reel, mm; h_0 is the stubble height of rape, 350 mm; h_1 is the height of rape plant, 1818 mm; R_b is selected as reel radius, 450 mm.

In order to ensure that the reel can push rape plants stably, the action point of the reel should be slightly higher than the center of gravity of the cut rape, namely:

$$H_b \geq R_b + \frac{2}{3}(h_1 - h_0).$$

In view of the unique nature of rape material, when analyzing the installation height when the reel vertically enters the crop, it can be determined that H_b = 1749 mm. On the premise of ensuring stable pushing, the installation height $H_b \geq$ 1429 mm. After comprehensive consideration, H_b = 1750 mm is adopted as the installation height of reel in this study. In addition, in order to ensure that when the reel is directly above the cutter, the reel rod still has the function of pushing backward, it is necessary to meet the horizontal distance relationship between the cutter and the reel spindle as follows:

$$B_b = \frac{D_b}{2\lambda\sqrt{\lambda^2-1}}.$$

Calculated B_b = 225.1 mm.

2.3.2. Cutting device design

The main function of the windrower cutter is to cut the Rape Stalk. In this paper, the reciprocating cutter with high efficiency and strong adaptability is selected, and its cutting parameters should meet the following requirements:

$$s = t = t_0 = 76.2mm,$$

where s is the cutter stroke, mm; t is the moving blade pitch, mm; t_0 is the blade guard pitch, mm.

The cutting speed of rape harvesting is generally 0.8~1.2 m/s [11]. If the initial cutter speed is 1 m/s, the crank speed is:

$$n_q = \frac{15v_d}{r_d},$$

where n_q is the crank speed of reciprocating cutter, r/min; v_d is the cutting speed of reciprocating cutter, m/s; r_d is the crank radius of reciprocating cutter, 38.1 mm.

The calculated crank speed n_q = 395 r/min.

2.3.3. Conveyor design and analysis

The main function of the conveyor mechanism of the windrower is to effectively transport the cut rape from both sides of the header to the grain discharge opening, and at the same time prevent the rape from being crushed. The single structure of the header is composed of two conveying parts on the left and right, which are arranged on both sides of the header in an inclined manner, and the gap in the middle is the row mouth. The transportation process of rape is completed by shifting the spring teeth on the conveyor belt to the center.

In the design of the rubber sleeve of the conveying mechanism, its diameter is determined to be 100 mm. The effective length of the outer belt is set at 800 mm, while the effective length of the inner belt is set at 1200 mm. In order to ensure that the cut rape can fall on the conveyor belt as much as possible, and considering the length limit of the header, the longitudinal length of the conveyor belt is set to 1000 mm. In addition, in order to ensure that the rape can be transported smoothly after being cut down, the ratio β between the linear speed of the conveyor belt and the forward speed of the unit is set at 1.4 [12]. It is concluded that:

$$\beta = \frac{v_s}{v_m} = \frac{2\pi R_s n_s}{60v_m},$$

where n_s is the rotational speed of the driving shaft of the conveyor belt, r/min; v_m is the forward operation speed of the unit, 1 m/s; v_s is the linear speed of belt rotation, m/s; R_s is the radius of rubber sleeve, 50 mm.

The calculation shows that the rotational speed of the driving shaft of the conveyor belt is n_s = 260 r/min.

2.4. Topology optimization design of harvester header device frame

2.4.1. Establishment of finite element model

In the process of exploring the structural complexity of rape windrower to improve the efficiency of simulation calculation, the necessary simplification of non key characteristics in the model is implemented. The header device of the windrower includes a header support and a hydraulic folding hanger. Based on their functional structural characteristics, the geometric models of the header support and the folding hanger are constructed, as shown in **Figure 2**. In this model, the positions marked I, II and III represent the constraint points, while the positions numbered 1 to 7 represent the positions where the load is applied. When performing finite element analysis, mesh quality has a decisive impact on the efficiency and accuracy of the solution, so the mesh generation must meet the standards of coordination, compatibility and accurate approximation. In view of the regularity of the rack structure, the tetrahedral grid is selected to divide the main body of the rack in this study to improve the computational efficiency [13]. Then, the two rack models were imported into the static structural module of ANSYS software respectively, and the material properties were set to Q235. The main part used 10 mm tetrahedral grid units, and the grid encryption was implemented in key parts to ensure that the quality of the grid met the analysis requirements.

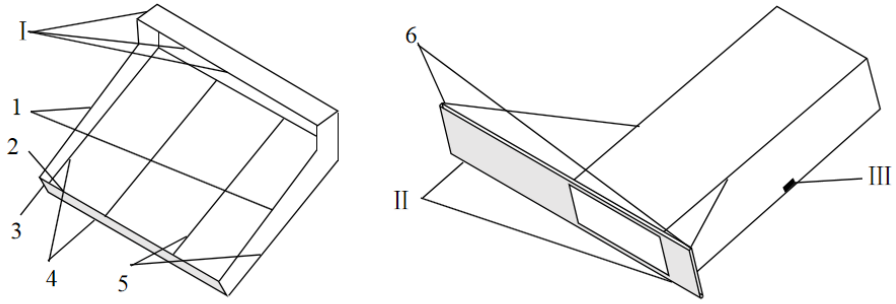

Initial model of the cutting platform　　Initial model of folding suspension frame

Ⅰ. Cutting table hanging point Ⅱ. Folding device handover point Ⅲ. Folding device rotation position 1. Installation point for the pulling wheel 2. Horizontal cutting blade installation beam 3. Vertical cutting blade installation beam 4. Installation beam of intermediate conveying device 5. Installation beam of side conveyor device 6. Cutting table hanging point

Figure 2. Initial model for topology optimization.

2.4.2. Load and constraint analysis

In the structural analysis of the header frame, it mainly bears the mechanical action caused by the gravity of each component. In view of the poor working condition of the windrower in the actual operation and transfer process, the mass and basic load of the header frame must be multiplied by the dynamic load coefficient for correction [14]. When the header is deployed, the header frame benefits from the supporting force of the hydraulic folding device and the pulling force of the folding hydraulic cylinder. It can impose fixed constraints on the attachment hinge of the header and the ear base of the hydraulic cylinder, introduce the gravity acceleration in the negative direction along the *Y* axis, and apply the equivalent load equivalent to the working part. When the header is folded, the position of the header hitch hinge and the ear base at the lower end of the hydraulic cylinder is still subject to fixed constraints. At this time, the gravity acceleration is adjusted along the positive direction of the *X* axis, and the load borne by the rack remains unchanged, but the direction rotates by

90°.

In this study, the vertical downward dynamic load coefficient is set as 2.5, and the gravity acceleration g = −9.8 m/s^2 is used as the analysis basis. In addition to bearing its own weight, the folding hanger is also mainly subject to the balanced force generated by the gravity of the left and right headers. These forces act on both sides of the crossbeam in front of the folding hanger, with the same size and direction. The fixed constraints of the folding suspension frame are mainly located at the front hydraulic cylinder ear and the rotating shaft. According to the above settings, the load data of header frame and folding hanger are shown in **Table 2**.

Table 2. Main loads borne by the cutting platform and folding suspension frame.

Main components		Mass (kg)	Load (N)	Load position
Cutting frame	Pulling wheel	47.4	1160.3	1
	Horizontal cutting knife	21.4	524.3	2
	Vertical cutting knife	8.1	198.5	3
	Small conveying device	28.3	695.0	4
	Large conveying device	33.1	811.0	5
Folding suspension rack	Left cutting platform	295	7227.5	6
	Right cutting table	295	7227.5	7

2.4.3. Topology optimization design of header frame

Before the topology optimization design, the original model must be imported into the ANSYS static structural module to perform the static analysis. In this process, the corresponding constraints and loads need to be applied [15]. After completing the static analysis, it is necessary to link the analysis results with the topology optimization module, then define the objective function and optimization area, and impose manufacturing reservation constraints on the functional structure. In this study, the stiffness of the structure is maximized as the objective function, the initial shell structure model is divided into finite element grids, and the variable density method is used to optimize the topology of the continuum to determine whether the elements in the design area are retained or not [16]. According to the material removal rate of 70%–95%, set a level every 5%, and carry out a series of simulation analysis. In the area where the structural form of the model is sensitive to the change of removal rate, additional experimental groups are added in this study. After topology optimization, the design scheme with significant structural difference and suitable for engineering application is selected from the results. As shown in **Figure 3**, the optimal design of the header frame in the expanded and folded state is shown. In the expanded state, the design schemes with 90%, 95% and 97% of the initial model material removal rate have significant differences in structural morphology, and meet the actual processing requirements. In the folded state, the design schemes with material removal rates of 80%, 85% and 90% also show significant differences in structural morphology, and all meet the actual processing standards.

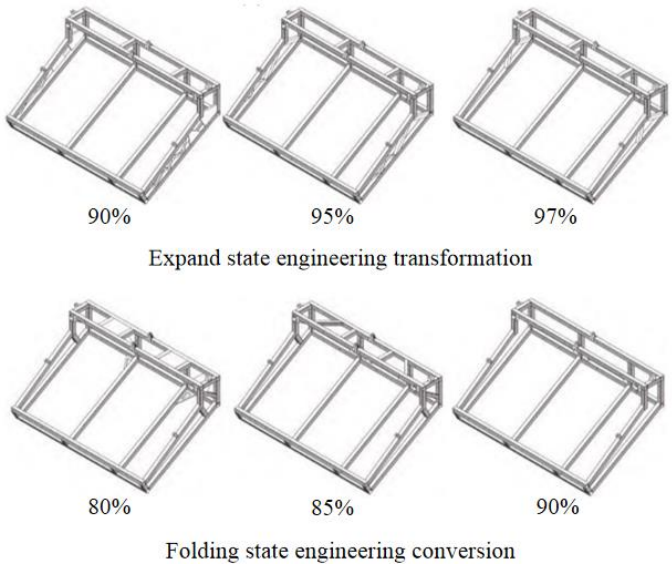

Figure 3. Topological structure and engineering transformation of the cutting platform.

Taking mass, maximum stress and maximum deformation as the core evaluation criteria, different design schemes of header frame are compared, and the relevant parameters are shown in **Table 3**. In view of the fact that the header frame needs to meet the strength requirements in both the unfolded and folded states, this study adopted the optimization scheme of 95% removal rate in the unfolded state and 85% removal rate in the folded state as the basis for further optimization.

Table 3. Parameters of various engineering schemes for the cutting platform.

Optimize conditions	Removal rate (%)	Mass (kg)	Maximum stress (Mpa)	Maximum deformation (mm)
Expand Status	90	107.91	107.28	0.92
	95	96.78	131.52	3.31
	97	95.11	194.33	3.69
Folding state	80	90.7	220.25	1.86
	85	97.39	150.81	5.11
	90	115.23	119.36	1.07

3. Results and analysis

3.1. Modal optimization effect of header frame

The purpose of this study is to evaluate the performance of the reconstructed header frame model, and the finite element analysis software is used to simulate the frame. In the simulation process, the primary natural frequency and stiffness of the reconstructed header frame are analyzed, and the boundary conditions set are consistent with the parameters of the topology optimization model. As shown in **Table 4** and **Figure 4**, the modal analysis results before and after optimization are in sharp contrast. After optimization, the first three natural frequencies of the header are increased, especially the first natural frequency is increased to 25.60 Hz, which effectively avoids the frequency bifurcation of vibration excitation and engine

excitation generated in the operation of working parts, reduces the risk of resonance, so as to optimize the dynamic performance of the header, and proves the effectiveness of the optimization strategy.

Table 4. Modal analysis results before and after optimization.

Order number	Natural frequency before optimization	Optimized natural frequency
1	18.65	25.60***
2	24.51	42.35***
3	32.04	44.80***
4	60.88	55.82***
5	64.23	63.14
6	78.98	70.88***

Note: * $p < 0.05$; ** $p < 0.01$; *** $p < 0.00$.

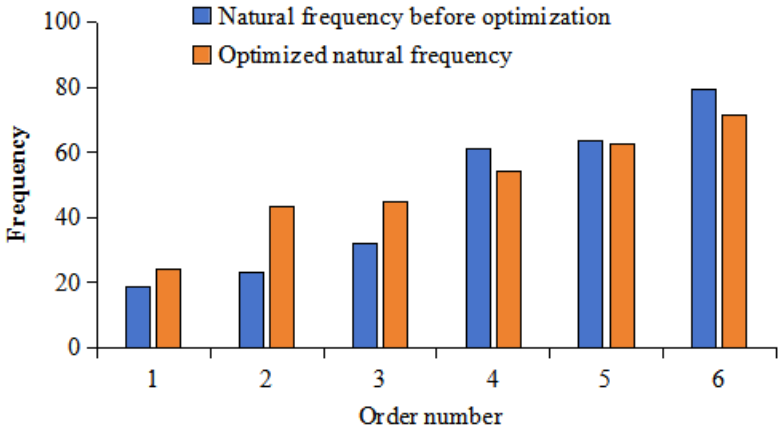

Figure 4. Modal analysis results before and after optimization.

3.2. Header vibration test

The purpose of this study is to compare the amplitude difference of the rape windrower header before and after optimization under the same working conditions. The vibration test was carried out in Ili Kazakh Autonomous Prefecture area on 16 May 2024. The header vibration test system is composed of dh-5902 dynamic signal acquisition instrument, three-axis acceleration sensor (1a314e) and personal computer (PC) processing terminal. According to the sampling theorem, the sampling frequency should not be less than twice the frequency of the signal to be analyzed [17], so the sampling frequency is set to 500 Hz and the sampling duration is set to 60 s in this test. In order to ensure the accuracy and rationality of the collected data, the selected measuring points are designed to comprehensively reflect the overall vibration, local vibration and large deformation area of the header. For this reason, the measuring points are mainly arranged at the key parts of the connection between the header and the excitation source, including the transverse cutter support (measuring point 1), the longitudinal cutter support (measuring point 2), the conveyor support (measuring point 3), and the connection between the header beam and the chassis (measuring point 4). During the test, the forward direction of the whole machine is defined as the *X* axis, the left and right movement direction is defined as the *Y* axis, and the direction perpendicular to the ground is defined as the *Z* axis. See **Table 5** for specific header

vibration test conditions.

Table 5. Operating conditions of cutting table vibration experiment.

Experimental conditions	Machine operating status	Engine speed (r/min)	Speed (km/h)	Road conditions
1	Only engine operation	2200	0	Cement road
2	The engine and working components work simultaneously	2200	0	Cement road
3	Only engine operation	2200	3	Cement road
4	Only engine operation	2200	3	Mud road

The results of the operating condition test are shown in **Table 6** and **Figure 5**. The amplitude variation of measuring point 4 is relatively stable under different operating conditions, and the optimized amplitude variation is significant. This is mainly due to the natural frequency of the optimized cutting platform avoiding the secondary frequency of engine excitation (18.4 Hz), effectively avoiding resonance phenomena and reducing amplitude. In condition 2, the amplitude of the cutting table of both generations of prototypes exceeded that of other conditions, indicating that the working components have a greater effect on the vibration of the cutting table than road excitation. In addition, the amplitude of measuring point 2 (4.63, 1.52 m/s^2) is more significant than other monitoring points, confirming the main excitation effect of the longitudinal cutter in the vibration of the cutting table. By comparing the conditions of working condition 3 and working condition 4, it can be seen that the road surface in the field is relatively soft, which helps to absorb some of the impact and reduce the amplitude of each monitoring point during the operation of the sun cutter; After optimization, the amplitude of measuring point 1 before and after optimization decreased by 43.6% and 49.1% respectively under two working conditions, confirming the importance of road surface excitation on the vibration of the cutting platform. The optimization measures significantly improved the vibration amplitude of the cutting table, and the amplitude of each monitoring point was significantly reduced.

Table 6. Root-mean-square acceleration of total vibration at measurement points.

Experimental conditions	Measurement point 1		Measurement point 2		Measurement point 3		Measurement point 4	
	Before optimization	After optimization	Before optimization	After optimization	Before optimization	After optimization	Before optimization	After optimization
1	2.54	0.67^{***}	1.63	1.16^{*}	2.98	0.55^{***}	1.96	0.32^{**}
2	3.86	0.92^{***}	4.63	1.52^{***}	3.32	0.98^{***}	2.54	0.53^{***}
3	2.98	0.55^{***}	2.83	0.54^{***}	2.67	0.61^{***}	2.58	0.42^{***}
4	1.68	0.28^{***}	1.54	0.41^{**}	2.22	0.57^{***}	2.33	0.42^{***}

Note: * $p < 0.05$; ** $p < 0.01$; *** $p < 0.00$.

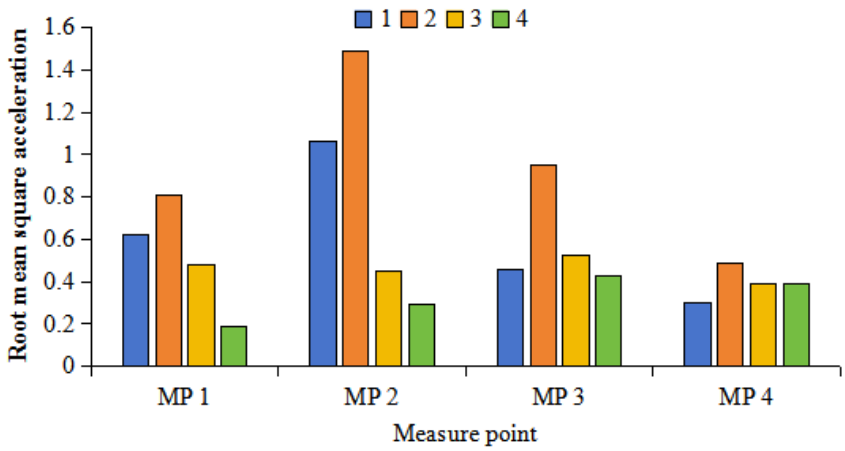

Figure 5. Root-mean-square acceleration of optimized measurement point vibration total.

4. Discussion

This article takes the rapeseed track type sun cutting machine cutting table as the research object, analyzes the basic structure and working process of the sun cutting machine cutting table, and through biomechanical analysis of the pulling, cutting and other links, accurately grasps the interaction mechanism between rapeseed and cutting table components, providing key basis for component design optimization. The analysis method combining vibration modes was used to obtain the vibration amplitude and frequency distribution of the rapeseed cutting table, and the main factors affecting its vibration were analyzed. The topology optimization of the cutting platform takes stiffness as the objective function, and through finite element analysis and multiple experiments, the engineering scheme with an initial model removal rate of 85% for the platform and an initial model material removal rate of 80% for the folding suspension frame is determined. After optimization, the natural frequency was found to have increased, effectively avoiding resonance. For example, the first natural frequency was significantly increased, enhancing the dynamic stability of the cutting table and reducing the impact of vibration on operational accuracy and mechanical life, laying the foundation for the long-term stable operation of the sun cutting machine.

This study comprehensively optimizes the efficiency of the rapeseed track type sun cutting machine cutting platform, effectively solves practical problems, improves the efficiency and quality of rapeseed harvesting, increases farmers' income, and effectively promotes the progress of rapeseed mechanized harvesting technology. It is of great significance for improving the overall level of agricultural mechanization in China and promoting the process of agricultural modernization, and provides a reference example for related research and improvement in the field of agricultural machinery.

Author contributions: Conceptualization, XT and JG; methodology, JM; software, XT; validation, XT, JG and JM; formal analysis, XT; investigation, XT; resources, XT; data curation, JM; writing—original draft preparation, XT; writing—review and editing, JG; visualization, JM; supervision, JG; project administration, XT; funding acquisition, JM. All authors have read and agreed to the published version of the

manuscript.

Ethical approval: Not applicable.

Conflict of interest: The authors declare no conflict of interest.

References

1. Du CF. Development status of rapeseed varieties and efficient planting techniques for high-quality seeds. China Farmers' Cooperative; 2022.
2. Gan GY, Zou JL, Chen X, et al. Research Status of Rapeseed Production Pattern and Fertilization in China. Hubei Agricultural Science; 2022.
3. Li P, Liao QX, Shu CX, et al. Analysis of Failure Causes and Parameter Matching Study on Stem Laying Quality of Rapeseed Harvester. Journal of Applied Basic and Engineering Sciences. 2016.
4. Upadhyay G, Kumar N, Raheman H, et al. Predicting the Power Requirement of Agricultural Machinery Using ANN and Regression Models and the Optimization of Parameters Using an ANN–PSO Technique. AgriEngineering. 2024; 6(1): 185-204. doi: 10.3390/agriengineering6010012
5. Zhang J, Hu Z, Zhou X, et al. Intelligent Controlling Model for Cleaning of Rice–Wheat Combine Harvester Based on Multi-Objective Optimization Particle Swarm Method. International Journal of Pattern Recognition and Artificial Intelligence. 2024; 38(06). doi: 10.1142/s0218001424510108
6. Liu YP. Research on the Impact of Optimizing Operating Parameters of Agricultural Plant Protection Machinery on the Ecological Environment of Farmland. Southern Agricultural Machinery; 2024.
7. Zhao SJ, Lu CY, Li SZ, et al. Optimization and Testing of the Performance of Kiwi Inter Plant Mechanical Obstacle Avoidance Weeding Machine. Agricultural Mechanization Research; 2023.
8. Singh G, Tewari VK, Potdar RR, et al. Modeling and optimization using artificial neural network and genetic algorithm of self-propelled machine reach envelope. Journal of Field Robotics. 2023; 41(7): 2373-2383. doi: 10.1002/rob.22255
9. Min Z, Bo Y, Wei L, et al. Simulation optimization and experimental validation of hydraulic impact in pruning machines. Measurement Science and Technology. 2024; 36(1): 015305. doi: 10.1088/1361-6501/ad8bea
10. Emberger P, Hinrichs M, Huber G, et al. Field tests and real-world exhaust gas emissions of a pure rapeseed oil-fuelled harvester in forestry: Testing a solution for combined water, soil, and climate protection. Journal of Cleaner Production. 2021; 280: 124360. doi: 10.1016/j.jclepro.2020.124360
11. Zhang JZ, Wang B, Zeng WG, et al. Research on the Most Unstable Attitude of Crawler Excavators under Slope Operating Conditions. Coal Mining Machinery; 2022.
12. Duan ZK. Optimization Design of Chassis System for Tracked Green Feed Harvester. Mechanical Research and Application; 2019.
13. Wang GH, Lei LY, Hu F. Optimization analysis of dual-purpose pickups for full feed combine harvesters and balers. Jiangsu Agricultural Mechanization; 2019.
14. Paraforos DS, Griepentrog HW. Switching Markov chains for modelling the loads of a four-rotor swather under different operating modes. IFAC-PapersOnLine. 2017; 50(1): 5392-5397. doi: 10.1016/j.ifacol.2017.08.1072
15. Sethanan K, Neungmatcha W. Multi-objective particle swarm optimization for mechanical harvester route planning of sugarcane field operations. European Journal of Operational Research. 2016; 252(3): 969-984. doi: 10.1016/j.ejor.2016.01.043
16. Khalil K, Mohd A, Mohamad COC, et al. The Optimization of Machining Parameters on Surface Roughness for AISI D3 Steel. Journal of Physics: Conference Series. 2021; 1874(1): 012063. doi: 10.1088/1742-6596/1874/1/012063
17. Feng W, Zhou TJ, Zhao HB, et al. Effect of Al content on microstructure and high temperature tensile properties of high wolfram cast superalloy. Heat Treatment of Metals. 2016; 41(7): 21-24. doi: 10.13251/j.issn.0254-6051.2016.07.005.